Biochemical and Biophysical Research Communications 418 (2012) 475–482

Contents lists available at SciVerse ScienceDirect

Biochemical and Biophysical Research Communications

journal homepage: www.elsevier.com/locate/ybbrc

Functional elements demarcated by histone modifications in breast cancer cells

Moon Kyung Choe [a,1], Chang-Pyo Hong [a,1], Jihwan Park [a], Seong Hye Seo [a], Tae-Young Roh [a,b,*]

[a] Division of Molecular and Life Sciences, POSTECH (Pohang University of Science and Technology), Pohang, Kyungbuk 790-784, Republic of Korea
[b] Division of Integrative Biosciences and Biotechnology, POSTECH (Pohang University of Science and Technology), Pohang, Kyungbuk 790-784, Republic of Korea

ARTICLE INFO

Article history:
Received 29 December 2011
Available online 20 January 2012

Keywords:
Breast cancer
Histone modification
Epigenome
Regulatory elements
Enhancer

ABSTRACT

Histone modifications are regarded as one of markers to identify regulatory elements which are DNA segments modulating gene transcription. Aberrant changes of histone modification levels are frequently observed in cancer. We have employed ChIP-Seq to identify regulatory elements in human breast cancer cell line, MCF-7 by comparing histone modification patterns of H3K4me1, H3K4me3, and H3K9/14ac to those in normal mammary epithelial cell line, MCF-10A. The genome-wide analysis shows that H3K4me3 and H3K9/14ac are highly enriched at promoter regions and H3K4me1 has a relatively broad distribution over proximity of TSSs as well as other genomic regions. We identified that many differentially expressed genes in MCF-7 have divergent histone modification patterns. To understand the functional roles of distinctively histone-modified regions, we selected 35 genomic regions marked by at least one histone modification and located from 3 to 10 kb upstream of TSS in both MCF-7 and MCF-10A and assessed their transcriptional activities. About 66% and 60% of selected regions in MCF-7 and MCF-10A, respectively, enhanced the transcriptional activity. Interestingly, most regions marked by H3K4me1 exhibited an enhancer activity. Regions with two or more kinds of histone modifications did show varying activities. In conclusion, our data reflects that comprehensive analysis of histone modification profiles under cell type-specific chromatin environment should provide a better chance for defining functional regulatory elements in the genome.

1. Introduction

The hierarchical folded structure of eukaryotic DNA forms nucleosome, chromatin fiber, and eventually chromosome in the nucleus [1]. A nucleosome, basic unit of chromatin consists of two copies of four core histones (H2A, H2B, H3, and H4) wrapped by 146 bp of DNA [2]. The N-terminal tails of histones are subject to various types of post-translational modifications such as acetylation, methylation, phosphorylation, ubiquitination, glycosylation, and sumoylation [3]. The dynamic addition and removal of these modifications carried out by histone modifying enzymes have been known to affect changes of chromatin structure so as to provide binding sites for proteins and to modulate cellular processes such as transcription, repair, replication, and genome stability [4–7]. Many genome-wide approaches to profiling histone modifications, especially ChIP-Seq, have revealed the characteristic genomic distribution and the association of gene functions and activities in various model organisms [8–14]. For example, H3K4me3 and many histone acetylations usually exist in promoter regions and positively correlated with gene transcriptional levels. Trimethylation of H3K27 is likely to spread over larger regions around TSSs of silent genes. The signals of trimethylations of H3K9 and H4K20 are high in silent genes and repressed chromatin domains. Many histone acetylation patterns are site-specific along the whole genome and are linked to transcriptional activation more or less [12,15]. The comprehensive analysis of many histone modifications in the human genome demonstrates that the combination of several histone modifications forms a modular pattern and influences transcriptional activation in a cooperative manner [15,16].

The availability of many genomic sequences from different organisms facilitates the discovery of functionally significant sequences by comparative genomics approach. However, the sequence comparison and mathematical modeling are not sufficient for discrimination of all functional elements from the bulk of the genome [17]. Besides evolutionary conserved sequences, many functional elements could be found by examining chromatin accessibility and histone modification or DNA methylation patterns [18–23]. A representative international project aiming to find all functional elements in the human genome called the Encyclopedia of DNA Elements (ENCODE) pilot project has examined about 1%

Abbreviations: H3K4me1, histone H3 Lysine 4 trimethylation; H3K4me3, histone H3 Lysine 4 monomethylation; H3K9/14ac, histone H3 Lysine 9 and 14 acetylation; TSS, transcription start site; TES, transcription end site; ChIP, chromatin immunoprecipitation.

* Corresponding author at: Division of Molecular and Life Sciences, POSTECH (Pohang University of Science and Technology), Hyojadong San 31, Namgu, Pohang, Kyungbuk 790-784, Republic of Korea. Fax: +82 54 279 8179.
E-mail address: tyroh@postech.edu (T.-Y. Roh).

[1] These authors contributed equally to this project.

0006-291X/
doi:10.1016/j.bbrc.2012.01.042

of human genomic sequences using a number of existing techniques [24]. Many functional elements examined by the ENCODE project are likely unconstrained across mammalian evolution and comprise a large reservoir of functionally conserved but non-orthologous elements between species as well as lineage-specific elements. The histone modification mapping could provide highly informative signatures to the estimation of presence and activity of gene promoters and distal regulatory sites. For the prediction of enhancers located in the non-coding region and enhancing the promoter activity by forming loop structure, several groups have finished genome-wide mapping of histone acetylation and methylation, DNase I hypersensitive sites, and p300 binding sites [11–13,15,19–21,25]. But not all the predicted enhancer candidates were validated due to the absence of proper assay condition closely mimicking the *in vivo* environment.

Breast cancer is a heterogeneous and progressive disease known as the most common cancers among women [26]. For the purpose of early diagnosis and prognosis, finding tumor makers in breast cancer is important but at present, no markers are available for its early detection [27,28]. The most clinically useful tissue-based markers in breast cancer are steroid receptors, estrogen receptors, progesterone receptors and HER-2 [27,29]. The mutations of BRCA1 and BRCA2 are strong indicators of breast cancer development but their occurrence is rare, in less than one out of 1000 patients [27]. Obviously, the perturbation of well-regulated gene expression program by epigenetic malfunction or other reason affects deregulation of cellular network leading to a tumor progression. In breast cancer, the loss of H4K20me3 and elevation of histone H4 acetylation are associated with aberrant expression of DNMT1 and Suv4-20h2 [30]. To further understand epigenetic regulatory mechanism on gene expression through differential histone modifications in normal and breast cancer cells, we performed ChIP-Seq analysis of H3K4me1, H3K4me3, and H3K9/14ac. We identified 140,691 and 115,000 peaks for H3K4me1, 23,979 and 22,306 for H3K4me3, and 23,579 and 24,716 for H3K9/14ac, in MCF-7 and MCF-10A, respectively. We randomly selected 35 regions located several kb upstream of TSSs and measured their transcriptional activities by luciferase reporter assay. The majority of enhancer candidates examined (23/35, 21/35) enhanced the transcriptional activity both in MCF-7 and MCF-10A, respectively. Interestingly, about 23% (8/35) of candidates were dramatically activated (at least >5-fold) in MCF-7 compared to the same candidate sequences in MCF-10A, implying that the environment of each enhancer is specific to cell types.

2. Materials and methods

2.1. Cell culture

MCF-7, an invasive ductal carcinoma cell line, was cultured in DMEM media supplied with 10% FBS and 50 U/ml penicillin and 50 μg/ml streptomycin. MCF10-A cells (ATCC, CRL-10317) were maintained in DMEM/F12 supplemented with 5% horse serum, 20 ng/ml EGF, 10 μg/ml insulin, 1 ng/ml cholera toxin, 100 μg/ml hydrocortisone, 50 U/ml penicillin, and 50 μg/ml streptomycin [31].

2.2. Preparation of chromatin and immunoprecipitation

After harvesting, 2×10^7 cells were suspended with 850 μl of ice-cold digestion buffer (50 mM Tris–HCl, pH 7.6, 1 mM $CaCl_2$, 0.2% Triton X-100, 5 mM butyrate, 1× proteinase inhibitor cocktail, and 0.5 mM fresh PMSF). The cells were incubated with 0.3 U of Micrococcal nuclease (Sigma, N3757) for 5 min at 37 °C and the reaction was stopped by adding 90 μl of 50 mM EDTA. The dialyzed mononucleosomes with RIPA buffer (10 mM Tris, pH 7.4, 1 mM EDTA, 0.1% SDS, 0.1% Na-Deoxycholate, 1% Triton X-100) were subject to immunoprecipitation with antibodies against H3K4me1 (Abcam, ab8895), H3K4me3 (Abcam, ab8580), H3K9/K14ac (Abcam, ab4441), and IgG (Santa Cruz, sc2025) [13]. After isolating ChIPed DNA, the efficiency and reproducibility of ChIP were validated by PCR.

2.3. Generation of sequencing library and ChIP-Seq analysis

Approximately 200 ng of ChIPed and input DNA were repaired using the End-It DNA End-repair kit (Epicentre Biotechnologies), followed by addition of 3′ A nucleotide for adaptor ligation. Overnight ligation of polished ChIPed DNA with Genomic DNA Adaptors from Illumina, amplification for 18 cycles, and isolation of about 220 bp from agarose gel were performed according to manufacturer's protocol. This ChIP-Seq library was sequenced by Illumina Genome Analyzer II. Sequence reads were aligned to human reference sequence (hg18) using CASABA 1.6 provided by Illumina. In MCF-7 cells, total mapped tag counts for H3K4me1, H3K4me3, H3K9/14ac, and input were 10.4, 2.2, 2.3, and 9.3 million reads, and in MCF-10A cells, 12.3, 9.8, 7.4, and 17.9 million reads, respectively. The normalized sequence reads were used for the further analysis [13]. The sequence data are deposited into the Sequence Read Archive (SRA) at the National Center for Biotechnical Information (NCBI) (SRA045635). To identify peaks enriched with a specific histone modification, the HOMER (Hypergeometric Optimization of Motif EnRichment) ver. 3.2 was used with the following options; approximate fragment length = 150 bp, peak size = 150 bp, minimum distance between peaks = 370 bp (equivalent to peak size ×2.5), Poisson *p*-value threshold relative to local tag count = 0.0001, default false discovery rate (FDR) threshold = 0.001, and center switch for centering peaks on maximum ChIP fragment overlap and calculating focus ratios [32]. The gene expression data using Affymetrix Human Genome U133 Plus 2.0 array platform was obtained from the Gene Expression Omnibus (GEO) at NCBI (GSM276046 ~ GSM276048 for MCF-7; GSM275995 ~ GSM275996 for MCF-10A) [33].

2.4. Luciferase reporter assay

Potential regulatory elements for measuring the transcriptional activities were selected on a basis of histone modification peak around 3–10 kb upstream of TSS (Supplementary Table S1). The regulatory element candidates ranging from 400 to 800 bp in length were amplified and cloned into the pGL3-HS vectors which were prepared by inserting minimal heat-shock promoter from pIND vector [34]. All cloned elements were confirmed by conventional DNA sequencing. One microgram of each reporter construct was transferred into both MCF-7 and MCF-10A cells using Genejuice transfection reagent (Novagen) following manufacturer's instruction. Cells were lysed 24 h after transfection and the luciferase activities at least in duplicate were measured using Dual-Luciferase Reporter Assay System (Promega). The regulatory element activities were normalized to basal activity of pGL3-HS vector.

3. Results

3.1. Genome-wide distribution of histone modification analyzed by ChIP-Seq

To map the genomic positions associated with H3K4me1, H3K4me3, and H3K9/14ac, we carried out ChIP-Seq analysis after validating ChIP efficiency and reproducibility by PCR (Supplementary Fig. S1). Using the HOMER, we identified 140,691 and 115,000 peaks of H3K4me1, 23,979 and 22,306 peaks of H3K4me3, 23,579 and 24,716 peaks of H3K9/14ac in MCF-7 and MCF-10A,

respectively (Supplementary Fig. S2). As shown in Fig. 1A, the H3K4me1 signals at promoters including 1 kb upstream and downstream of the TSS occupy 5% and 6% of the human genome in MCF-7 and MCF-10A, respectively, which is greater than that of the human genome (1%). The levels of H3K4me3 and H3K9/14ac at promoters are much higher in two cell types (23–30% of the genome) than those of H3K4me1. In particular, the highest peaks of H3K4me3 and H3K9/14ac appear at the immediate downstream of TSS, reflecting that the first nucleosome of genes is the major targets of these two modifications (Fig. 1B). The genomic enrichment of H3K4me1 is relatively broad near the TSS. The overall peak pattern of each modification in both MCF-7 and MCF-10A is quite similar. The peak distributions of histone modifications in Fig. 1C show that the H3K4me1 peaks are located in the exon, intron, 5′- and 3′-untranslated regions (UTRs), and even far upstream and downstream of genes. But most H3K4me3 and H3K9/14ac peaks are located in the 5′-UTR.

3.2. Correlation of histone modifications in MCF-7 and MCF-10A

To see whether the histone modifications in cancer and normal cells occurs at the same region, we calculated Pearson's correlation coefficients between two histone modification levels of all annotated genes' promoters, which are defined as log 2 values of sum of normalized tag counts detected within 1 kb upstream and downstream of TSS. As expected, the pair-wise correlation coefficients of H3K4me3 and H3K9/14ac in each cell type show the highest values, 0.86 and 0.90 in MCF-7 and MCF-10A, respectively (Fig. 2A). The correlation coefficients of the same histone modification in different cell types are 0.65 for H3K4me1, 0.59 for H3K4me3, and 0.70 for H3K9/14ac. The cross-coefficient of H3K4me3 in MCF-7 and H3K9/14ac in MCF-10A is 0.60 and that of H3K9/14ac in MCF-7 and H3K4me3 in MCF-10A is 0.67. The correlation of H3K4me3-H3K9/14ac in the same cell type (0.86 and 0.90) is more significant than that of H3K4me3-H3K9/14ac in

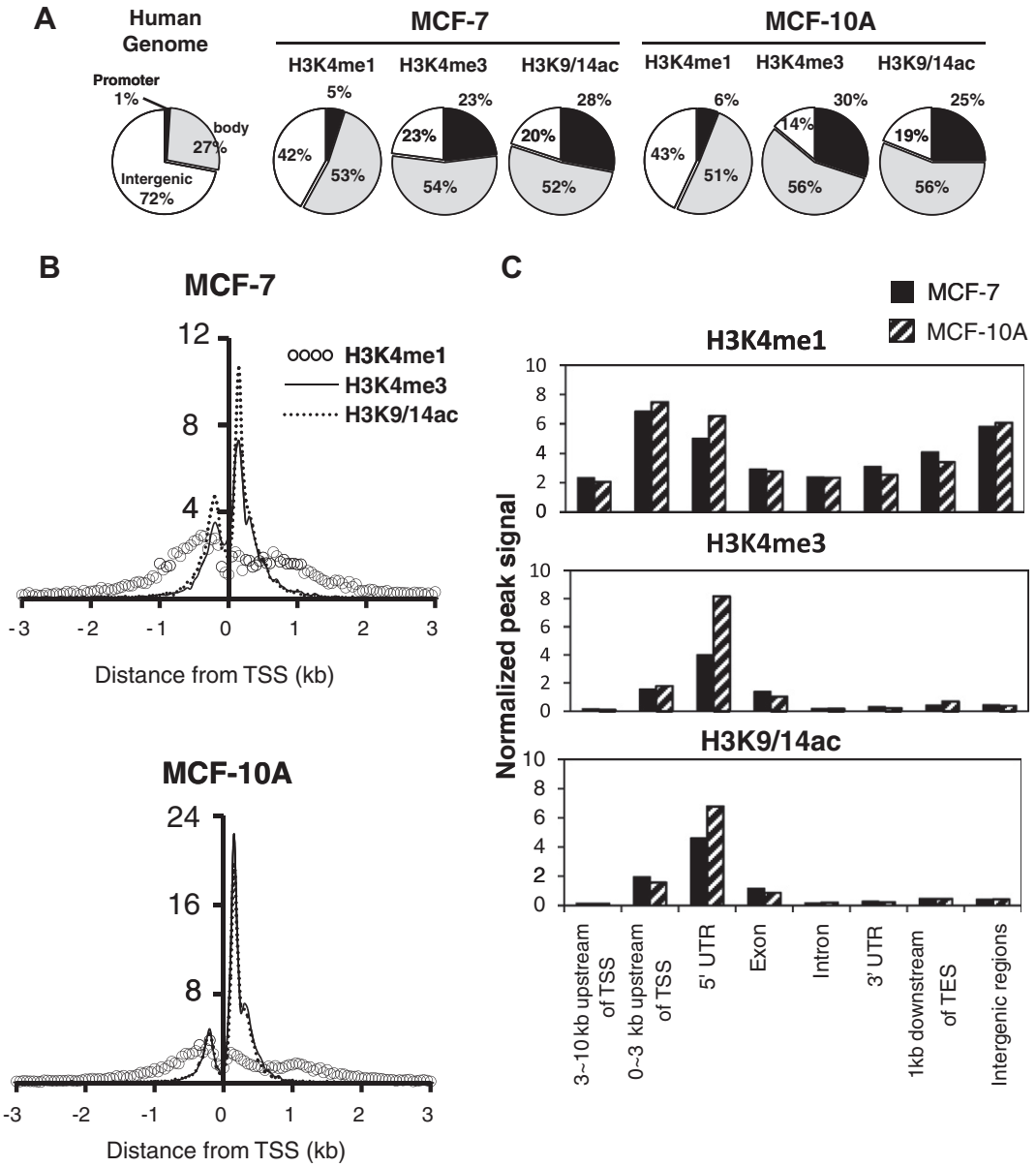

Fig. 1. Genome-wide occupancy of histone modifications in MCF-7 and MCF-10A. (A) The genomic distribution of histone modification peaks was calculated in promoter (±1 kb regions from TSS), gene body, and intergenic regions. The sequence allocation of human genome is shown on the left. (B) Profiles for the H3K4me1, H3K4me3, and H3K9/14ac were plotted ranging from −3 to +3 kb of the TSSs. The *Y* axis represents the normalized sum of peak counts, multiplied by 10,000. (C) Localization of histone modification peaks was shown in detail.

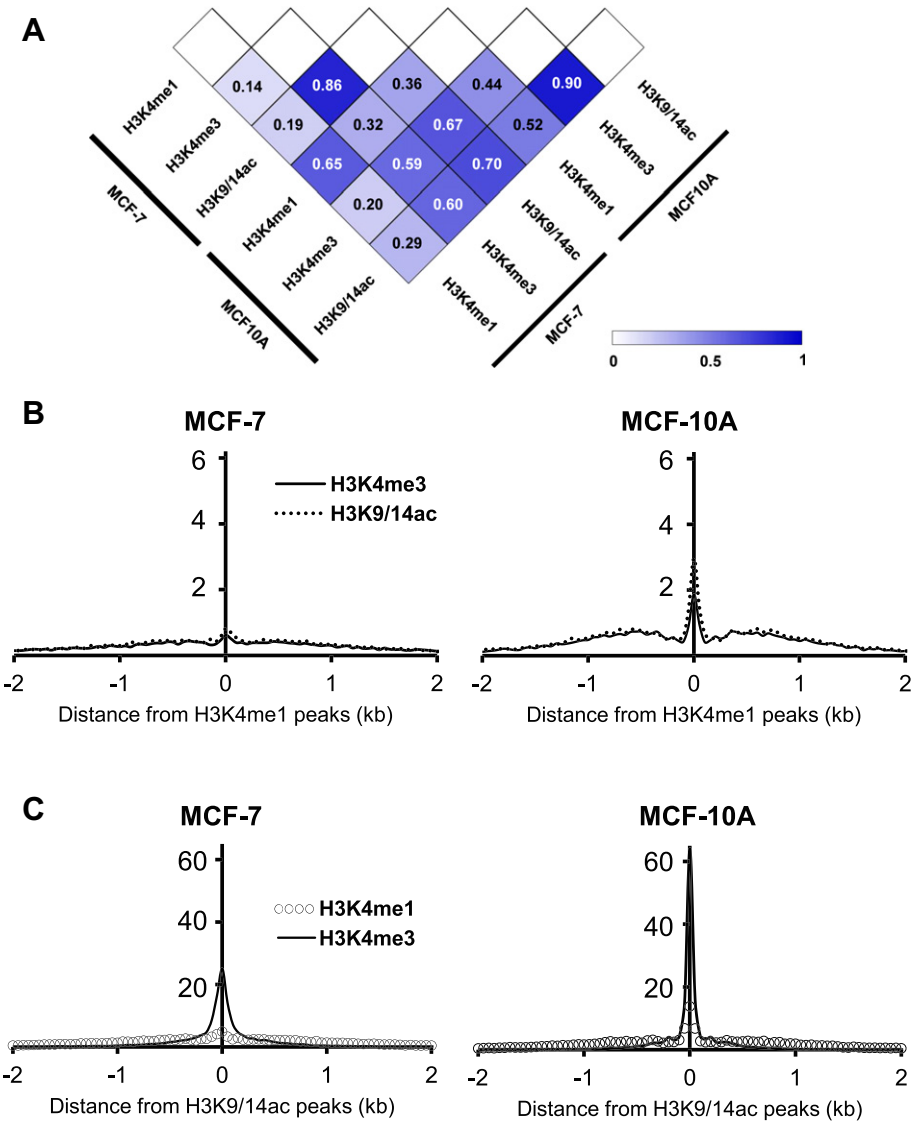

Fig. 2. Colocalization of histone modifications in MCF-7 and MCF-10A cells. (A) A heatmap was generated from Pearson's correlation coefficients for histone modification levels in the promoters. (B) The colocalization of H3K4me3 and H3K9/14ac peaks were analyzed centered on H3K4me1 peaks. (C) The colocalization of H3K4me1 and H3K4me3 peaks were analyzed centered on H3K9/14ac peaks. The *Y* axis indicates the normalized sum of peak counts, multiplied by 10,000.

different cell types (0.60 and 0.67) or that of the same modifications in different cell types (0.65, 0.59, and 0.70). The interaction of H3K4me1 with other histone modification is generally weaker in the promoter regions. The genome-wide correlations of H3K4me1 with H3K4me3 (0.003 for MCF-7 and 0.061 for MCF-10A) and H3K9/14ac (0.012 for MCF-7 and 0.152 for MCF-10A) are not as strong as those in the promoter regions. The colocalization of two histone modifications is shown in Fig. 2B and C where H3K4me1 or H3K9/14ac peaks are centered and the distribution of the other two histone modifications are plotted. When the distance between center positions of two peaks considered was shorter than 100 base pairs, two peaks were regarded as colocalized ones. In both MCF-7 and MCF-10A, the H3K9/14ac peaks are considerably overlapped with H3K4me3 but the H4K4me1 peaks are not.

3.3. Gene expression and histone modifications in MCF-7 and MCF-10A

To understand the relationship between histone modification and gene expression, we compared our ChIP-Seq data with the open source gene expression data for MCF-7 and MCF-10A. The gene expression levels are positively correlated with H3K4me3 ($R^2 = 0.6141$ and $R^2 = 0.9062$) and H3K9/14ac ($R^2 = 0.8869$ and $R^2 = 0.9374$) in MCF-7 and MCF-10A when plotted with 17,614 annotated genes (Fig. 3A, Supplementary Fig. S3). But the H3K4me1 signals exhibit relatively low correlation coefficients as previously reported [13]. In MCF-7 cells, the promoters of 2648 genes were more acetylated by at least 2-fold on H3K9/14 and the gene ontology (GO) analysis by the Database for Annotation, Visualization and Integrated Discovery (DAVID) tools revealed that they are associated with the following GO categories; DNA packaging, intracellular organelle lumen, cell morphogenesis, metal ion binding, regulation of cellular process, replisome, DNA processing, cell cycle, peroxisome, and transcription [35] (Supplementary Fig. S4). The functional classification was similar to that for up-regulated genes in MCF-7 cells (Supplementary Fig. S4). Interestingly, breast cancer-related genes up-regulated in MCF-7 are likely to have high level of H3K9/14ac. We identified 21 genes (DRD2, PRDM2, PTPRJ, CTCF, XRCC3, SULT1A1, AURKA, GSTZ1, MYCL1, BARD1, CDT1, CCND1, NCOA3, RAD51C, PRLR, IRS1, CXCL12, BRIP1, CALCR, CBS, and ESR1) from the cluster analysis of H3K9/14ac and expression of breast

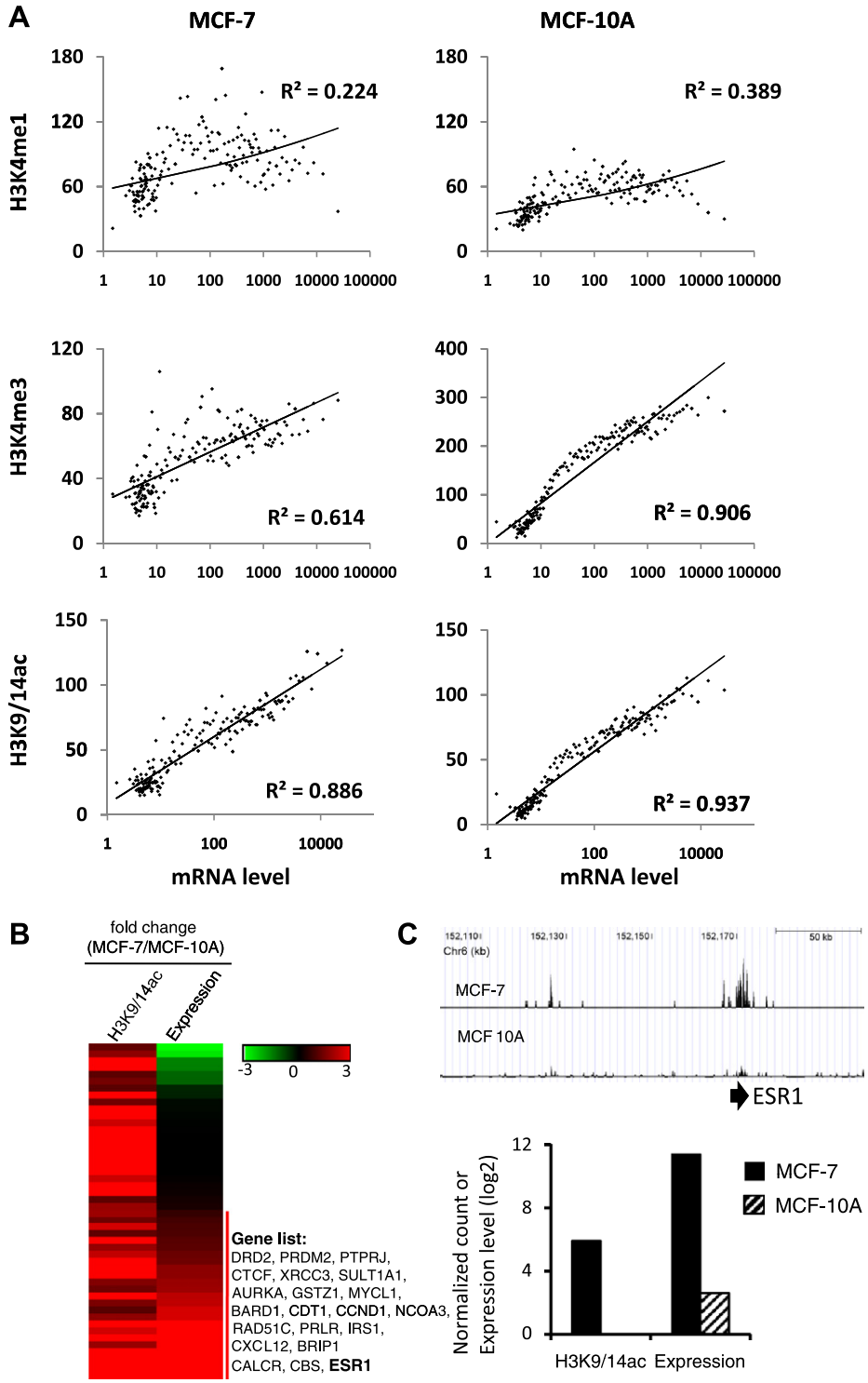

Fig. 3. Gene expression profiles and histone modifications. (A) The expression levels of 17,614 genes were compared to histone modification levels. Insets are regression coefficients (R^2). (B) A group of breast-cancer related genes were selected and calculated the fold changes of H3K9/14ac and expression levels. Genes were sorted by gene expression level. (C) The H3K9/14ac pattern for near ESR1 was shown and the TSS of ESR1 is denoted by arrow. The bar graph displays levels of H3K9/14ac and expression for ESR1.

cancer-related genes (Fig. 3B). For example, the promoter of estrogen receptor alpha (ESR1) is highly acetylated on H3K9/14ac and the over-expression of ESR1 is observed in MCF-7 (Fig. 3C).

3.4. Identification of regulatory elements in MCF-7 and MCF-10A

To find unknown regulatory elements which may enhance the promoter activity, we defined the histone modification peaks using the HOMER where significant peaks were determined by assuming that the local density of tags follows a Poisson distribution and calculating the expected number of false positives in the dataset for each tag threshold specified (FDR = 0.001) using the expected distribution of peaks (Supplementary Fig. S2 and an example (#5) in Supplementary Fig. S5). The histone modification peaks located about 3–10 kb upstream of TSS are shown in Fig. 4A where considerable number of peaks is not overlapped each other. Only a small

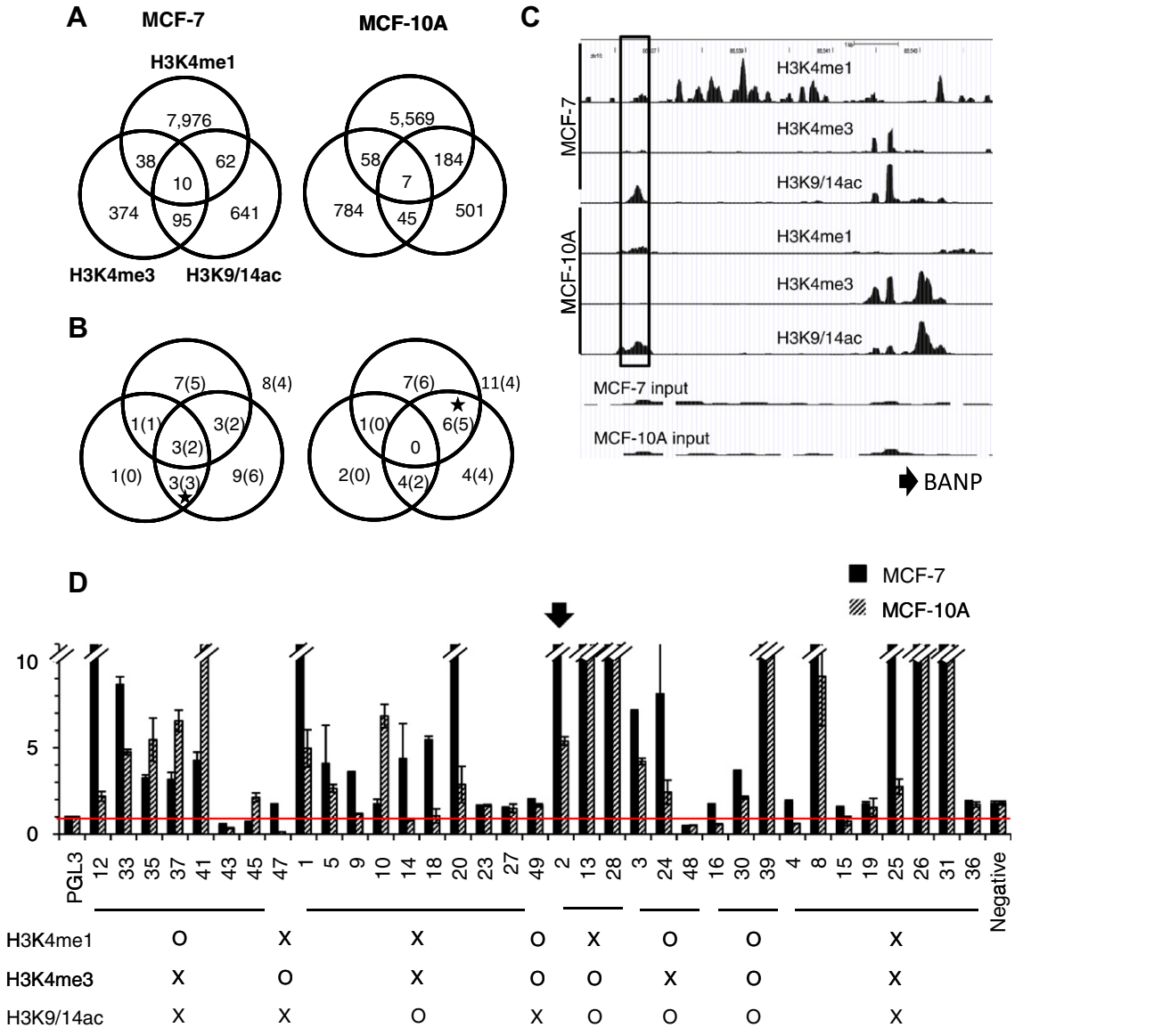

Fig. 4. Identification of regulatory element by the reporter assay. (A) The numbers of histone modification peaks within 3–10 kb upstream of TSS and their positional overlapping were examined in MCF-7 and MCF-10A cells. (B) The numbers of regulatory elements used for the reporter assay were listed and ones positively enhanced the transcriptional activity were shown in parenthesis. (C) The histone modification profiles upstream of BANP gene were examined. The boxed region was cloned for the reporter assay (clone #2), which belonged to the region marked by star in (B). (D) The transcriptional activities were determined by measuring the luciferase activity. Each bar represents the fold difference relative to the control vector (pGL3-HS). The 2-fold induction of luciferase activity was regarded as a threshold for determining the true activation. The *Y* axis indicates the fold activation.

portion of peaks (1.3% for H3K4me1, 28% for H3K4me3, and 21% for H3K9/14ac) is colocalized in the same chromatin region in MCF-7. Among them, only 10 peaks contain all three histone modifications. In MCF-10A, the overlapped peak ratios are 4.3%, 12.3%, and 32% for H3K4me1, H3K4me3, and H3K9/14ac, respectively. To explore the functional role of these histone modification peaks, we randomly selected 35 peak regions and tested transcriptional activity (Fig. 4B, Supplementary Table S1). An interesting example with differential H3K4me1 level in Fig. 4C is an upstream sequence of BTG3-associated nuclear protein (*BANP*) gene, a human homologue of tumor suppressor *SMAR1* which is one of p53 target genes [36]. Considering 11.9-fold enrichment of the reporter gene activity in MCF-7 and 5.4-fold in MCF-10A, this region (clone #2) can be regarded as a strong enhancer. Out of 35 potential regulatory elements, 23 candidates (66%) in MCF-7 and 21 (60%) in MCF-10A increased the reporter activity by at least 2-fold (Fig. 4D, Supplementary Table S1). As shown in Fig. 4B and D, the reporter assay revealed that 65% (11/17) and 77% (10/13) of monovalent potential enhancer elements exhibit elevated activities in MCF-7 and MCF-10A, respectively. The di- or trivalent elements also demonstrate high levels of activation, 80% (8/10) in MCF-7 and 64% (7/11) in MCF-10A. Interestingly, 50% (4/8) in MCF-7 and 36% (4/11) in MCF-10A are classified as enhancers even though they are not regarded as peaks by the HOMER. Even though the activities of the same element sequences were measured in both MCF-7 and MCF-10A, they showed divergent activities such that multivalent elements were likely to show higher activation than monovalent elements with some exceptions depending on cell type and chromatin environment. For example, clone #14 is activated by 5-fold in MCF-7 but not in MCF-10A.

4. Discussion

Like other cancers, breast cancer cannot be driven only by genetic abnormalities but also by epigenetic alterations [26,37,38]. In this study, we analyzed high-resolution distribution of H3K4me1, H3K4me1, and H3K9/14ac by ChIP-Seq in breast cancer cell, MCF-7 and normal cell, MCF-10A. As known previously, the promoter regions have high levels (>23%) of H3K4me3 and H3K9/14ac compared to 1% of genomic occupancy while H3K4me1 is pervasively distributed. We tried to find global differences in histone modification profiles between two cell lines but as seen in Fig. 1C, each region does not show significant changes, reflecting that histone modifications have their own propensity for binding to a specific region.

The pair-wise correlation study for H3K4me3 and H3K9/14ac indicates that these two modifications are greatly colocalized each other in the same cells but their correlation in different cells is moderate. The promoters with high levels of H3K4me3 also occupy elevated H3K9/14ac in one cell line. A comparison between two different cell types indicates that the correlations between H3K4me3-H3K4me3, H3K4me3-H3K9/14ac, and H3K9/14ac-H3K9/14ac are not as high as those in the same cells. This pair-wise correlation result is consistent with gene expression level shown in Fig. 3A where the gene expression levels are positively regulated by H3K4me3 and H3K9/14ac.

We examined histone modification patterns and gene expression level of breast cancer specific genes using DAVID Functional Annotation tool and identified 21 breast cancer-associated genes. The level of H3K9/14ac rather than H3K4me3 of these genes was well correlated with the degree of expression in MCF-7 (data not shown). The heat map analysis of H3K9/14ac and gene expression in MCF-7 demonstrates 21 plausible genes which are highly expressed, much acetylated, and especially related with breast cancer. These genes may be used as diagnostic markers if they are validated in a future experiment exploring in breast cancer patients.

The identification of cancer cell-specific functional elements is beneficial for early detection or prognostic improvement. We defined 140,691 and 115,000 H3K4me1 peaks in MCF-7 and MCF-10A. Because it was practically impossible to examine all peaks defined, we determined the following scope to assay selected peaks; (i) located in 3–10 kb distant from the TSS, (ii) equally distributed according to presence or absence of three histone modifications shown in Fig. 4A, and (iii) transfected successfully in both MCF-7 and MCF-10A. Apparently, over 60% of selected peaks increased the reporter gene activity and thus they might be regarded as enhancers even though stringent evaluation *in vivo* still remains. We tested only handful candidates for regulatory elements but the result was enough to shed a light on defining breast cancer cell-specific regulatory elements which could eventually be used as clinical markers. In summary, our approach in this study could make a meaningful contribution to identification of cell-type specific elements able to be used as a clue for understanding epigenetic alterations during disease progression.

Acknowledgments

We thank members of Lab. of System Genomics, POSTECH, for active discussion and Dr. Y.K. Shin, Seoul National University for kindly providing MCF-7. This work was supported by National Research Foundation (KRF-2008-313-C00665, 2010-0023412, and 2010-0026759), Korea Healthcare technology R&D Project, MHWFA (A084519), and the World Class University program, NRF, MEST (R31-10105), Republic of Korea.

Appendix A. Supplementary data

Supplementary data associated with this article can be found, in the online version, at doi:10.1016/j.bbrc.2012.01.042.

References

[1] B. van Steensel, Chromatin: constructing the big picture, EMBO J. 30 (2011) 1885–1895.
[2] K. Luger, A.W. Mader, R.K. Richmond, et al., Crystal structure of the nucleosome core particle at 2.8 A resolution, Nature 389 (1997) 251–260.
[3] T. Kouzarides, Chromatin modifications and their function, Cell 128 (2007) 693–705.
[4] R. Marmorstein, R.C. Trievel, Histone modifying enzymes: structures, mechanisms, and specificities, Biochim. Biophys. Acta 1789 (2009) 58–68.
[5] J.F. Couture, R.C. Trievel, Histone-modifying enzymes: encrypting an enigmatic epigenetic code, Curr. Opin. Struct. Biol. 16 (2006) 753–760.
[6] V.W. Zhou, A. Goren, B.E. Bernstein, Charting histone modifications and the functional organization of mammalian genomes, Nat. Rev. Genet. 12 (2011) 7–18.
[7] J.C. Black, J.R. Whetstine, Chromatin landscape: methylation beyond transcription, Epigenetics 6 (2011).
[8] D.K. Pokholok, C.T. Harbison, S. Levine, et al., Genome-wide map of nucleosome acetylation and methylation in yeast, Cell 122 (2005) 517–527.
[9] B.E. Bernstein, E.L. Humphrey, R.L. Erlich, et al., Methylation of histone H3 Lys 4 in coding regions of active genes, Proc. Natl. Acad. Sci. USA 99 (2002) 8695–8700.
[10] T.Y. Roh, W.C. Ngau, K. Cui, et al., High-resolution genome-wide mapping of histone modifications, Nat. Biotechnol. 22 (2004) 1013–1016.
[11] T.Y. Roh, S. Cuddapah, K. Cui, et al., The genomic landscape of histone modifications in human T cells, Proc. Natl. Acad. Sci. USA. 103 (2006) 15782–15787.
[12] T.Y. Roh, S. Cuddapah, K. Zhao, Active chromatin domains are defined by acetylation islands revealed by genome-wide mapping, Genes Dev. 19 (2005) 542–552.
[13] A. Barski, S. Cuddapah, K. Cui, et al., High-resolution profiling of histone methylations in the human genome, Cell 129 (2007) 823–837.
[14] D.E. Schones, K. Zhao, Genome-wide approaches to studying chromatin modifications, Nat. Rev. Genet. 9 (2008) 179–191.
[15] Z. Wang, C. Zang, J.A. Rosenfeld, et al., Combinatorial patterns of histone acetylations and methylations in the human genome, Nat. Genet. 40 (2008) 897–903.
[16] S.K. Kurdistani, S. Tavazoie, M. Grunstein, Mapping global histone acetylation patterns to gene expression, Cell 117 (2004) 721–733.
[17] E.A. Stone, G.M. Cooper, A. Sidow, Trade-offs in detecting evolutionarily constrained sequence by comparative genomics, Annu. Rev. Genomics Hum. Genet. 6 (2005) 143–164.
[18] R.K. Auerbach, G. Euskirchen, J. Rozowsky, et al., Mapping accessible chromatin regions using Sono-Seq, Proc. Natl. Acad. Sci. USA (2009).
[19] G.E. Crawford, I.E. Holt, J. Whittle, et al., Genome-wide mapping of DNase hypersensitive sites using massively parallel signature sequencing (MPSS), Genome Res. 16 (2006) 123–131.
[20] A. Visel, M.J. Blow, Z. Li, et al., ChIP-seq accurately predicts tissue-specific activity of enhancers, Nature 457 (2009) 854–858.
[21] N.D. Heintzman, G.C. Hon, R.D. Hawkins, et al., Histone modifications at human enhancers reflect global cell-type-specific gene expression, Nature 459 (2009) 108–112.
[22] K. Ishihara, M. Oshimura, M. Nakao, CTCF-dependent chromatin insulator is linked to epigenetic remodeling, Mol. Cell. 23 (2006) 733–742.
[23] P.A. Jones, D. Takai, The role of DNA methylation in mammalian epigenetics, Science 293 (2001) 1068–1070.
[24] E. Birney, J.A. Stamatoyannopoulos, A. Dutta, et al., Identification and analysis of functional elements in 1% of the human genome by the ENCODE pilot project, Nature 447 (2007) 799–816.
[25] T.K. Kim, M. Hemberg, J.M. Gray, et al., Widespread transcription at neuronal activity-regulated enhancers, Nature 465 (2010) 182–187.
[26] K. Polyak, Breast cancer: origins and evolution, J. Clin. Invest. 117 (2007) 3155–3163.
[27] P. Maric, P. Ozretic, S. Levanat, et al., Tumor markers in breast cancer–evaluation of their clinical usefulness, Coll. Antropol. 35 (2011) 241–247.
[28] B. Weigelt, J.L. Peterse, L.J. van 't Veer, Breast cancer metastasis: markers and models, Nat. Rev. Cancer 5 (2005) 591–602.
[29] M. Cianfrocca, W. Gradishar, New molecular classifications of breast cancer, CA Cancer J. Clin. 59 (2009) 303–313.
[30] V.P. Tryndyak, O. Kovalchuk, I.P. Pogribny, Loss of DNA methylation and histone H4 lysine 20 trimethylation in human breast cancer cells is associated with aberrant expression of DNA methyltransferase 1, Suv4-20h2 histone methyltransferase and methyl-binding proteins, Cancer Biol. Ther. 5 (2006) 65–70.
[31] M.J. Reginato, K.R. Mills, J.K. Paulus, et al., Integrins and EGFR coordinately regulate the pro-apoptotic protein Bim to prevent anoikis, Nat. Cell. Biol. 5 (2003) 733–740.

[32] S. Heinz, C. Benner, N. Spann, et al., Simple combinations of lineage-determining transcription factors prime cis-regulatory elements required for macrophage and B cell identities, Mol. Cell. 38 (2010) 576–589.

[33] S. Stinson, M.R. Lackner, A.T. Adai, et al., TRPS1 targeting by miR-221/222 promotes the epithelial-to-mesenchymal transition in breast cancer, Sci. Signal. 4 (2011) ra41.

[34] T.Y. Roh, G. Wei, C.M. Farrell, et al., Genome-wide prediction of conserved and nonconserved enhancers by histone acetylation patterns, Genome Res. 17 (2007) 74–81.

[35] W. Huang da, B.T. Sherman, R.A. Lempicki, Systematic and integrative analysis of large gene lists using DAVID bioinformatics resources, Nat. Protoc. 4 (2009) 44–57.

[36] K. Singh, D. Mogare, R.O. Giridharagopalan, et al., P53 target gene SMAR1 is dysregulated in breast cancer: its role in cancer cell migration and invasion, Plos One 2 (2007) e660.

[37] M. Widschwendter, P.A. Jones, DNA methylation and breast carcinogenesis, Oncogene 21 (2002) 5462–5482.

[38] P.K. Lo, S. Sukumar, Epigenomics and breast cancer, Pharmacogenomics 9 (2008) 1879–1902.